# Design of a Novel Bearingless Permanent Magnet Motor for Bioreactor Applications

Thomas Reichert[1], Thomas Nussbaumer[2], Wolfgang Gruber[3], Johann W. Kolar[1]

[1]Power Electronic Systems Laboratory, ETH Zurich, 8092 Zurich, Switzerland

[2]Levitronix GmbH, Technoparkstrasse 1, 8005 Zurich, Switzerland

[3]ACCM GmbH (Johannes Kepler University Linz), 4040 Linz, Austria

*reichert@lem.ee.ethz.ch*

*Abstract*-**The paper presents a novel topology for a bearingless permanent magnet motor. This disk-shaped motor can be advantageously employed in delicate bioreactor processes. Both torque and bearing forces originate inside this magnetically levitated motor. Using 3D-FEM analysis, the optimal machine sizing parameters are evaluated with the goal to maximize torque while providing sufficient bearing forces to allow a stable operation.**

## I.     INTRODUCTION

In technology sectors that ask for highly clean environment and gentle work procedures, the bearingless motor can be advantageous over a motor with a conventional bearing despite its higher cost and control effort [1]-[5]. Due to its magnetically levitated rotor this motor concept is completely wear- and lubrication-free. Therefore, this motor is highly qualified for the use in processes that take place inside hermetically sealed enclosures such as reactors, pumps, etc. Only the levitated rotor is placed inside the process room, whereas the stator and all the control electronics are placed outside (cf. Fig. 2).

The stirred vessel is the most commonly used type of bioreactor [6]-[8]. One or several agitators create a loop flow inside the vessel, which is necessary to constantly supply the cell culture with air bubbles and nutrition. The agitators can either be mounted from the bottom or from the top (requiring a longer shaft). Top-mounting however, significantly reduces the space for inlets and sensor mountings and requires large head space, wherefore in many applications bottom-mounted stirrers are preferred. The main requirement for the motor (agitator) of such a stirred bioreactor is a high torque at usually rather low rotation speeds [8]. State-of-the-art bioreactors either use an external motor with a long shaft passing through a sealed opening in the reactor wall (cf. Fig. 1), or the torque is transmitted by means of a magnetic coupling. However, both variants (seal and magnetic coupling) create pinch-off areas inside the vessel that harm the cell culture. A magnetically levitated motor requires no seals and has absolutely no direct contact with the reactor wall. Therefore, the impact on cell destruction can be significantly reduced. Moreover, the large possible air gap makes this motor suitable for clean-in-place (CIP) and sterilization-in-place (SIP) applications [9].
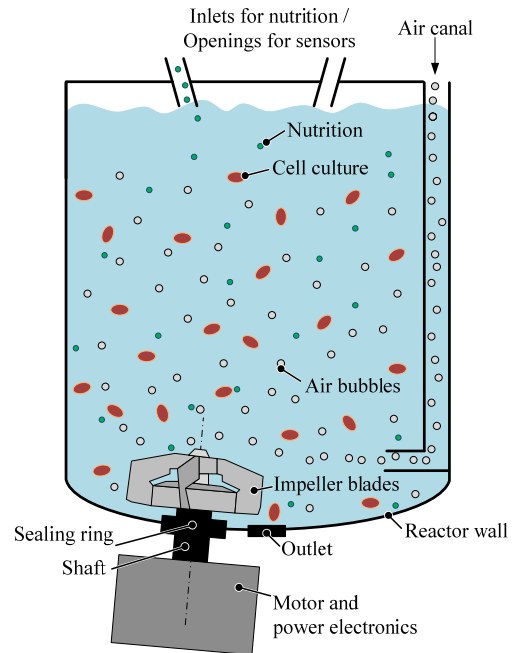


Fig. 1. Schematic view of a stirred vessel bioreactor with a single bottom-mounted agitator. The rotating seal creates a pinch-off area that can harm cell cultures.

In this paper, a novel bearingless motor topology consisting of an exterior disk-shaped rotor with a pole pair number of six and a stator with four stator teeth is introduced. In section II, the motor requirements are described and the selection of the motor setup is derived. Section III describes the combined torque and force production of this novel machine. With 3D magnetostatic FEM simulations, the optimal design is derived in section IV. Moreover, the optimal winding number per coil is analyzed. Finally, a prototype setup has been built for feasibility studies and verification of the simulations (see Section V).

## II.     SELECTION CRITERIA FOR MOTOR SETUP

In this paper, the focus lies on a bioreactor with a single bottom-mounted agitator. The outer diameter of the impeller depends on the size of the vessel. For the targeted bioreactor with a volume of 500 l, the outer diameter of the impeller is set to 170 mm. The air gap between stator and rotor needs to
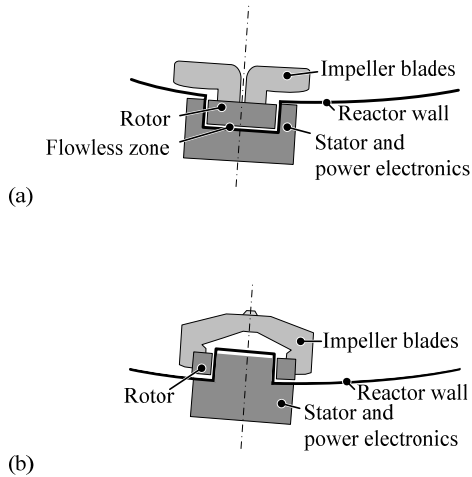
Fig. 2. Schematic view of a stirred vessel bioreactor with bottom-mounted bearingless motor. The interior-rotor type (a) creates unwanted flowless zones. Therefore, the exterior-rotor setup (b) is preferable. Only the rotor is placed inside the reactor and there is no need for seals or magnetic couplings.

be sufficiently large, so that the rotor has a certain distance from the reactor wall when levitating. For a wall thickness of 1 mm, the magnetical air gap thickness is set to 4 mm, so that there is sufficient space between the wall and the rotor when levitating. This is necessary to avoid pinch-off areas and for the CIP and SIP processes.

In a first step, the selection between interior and exterior rotor type motor has to be made. Fig. 2 compares the two concepts. In Fig. 2(a), the vessel is extended at the bottom so that the rotor can be placed inside and the stator around it. The impeller has to be fixed on top of the rotor, so that the impeller blades can be mounted higher inside the vessel allowing a higher agitation impact. However, this interior rotor setup bears a significant disadvantage. The flow will only slightly enter the extended bottom area, thus creating an undesired dead zone. Moreover, the required impeller impairs the stability of the magnetic bearing. Therefore, the exterior rotor type – depicted in Fig. 2(b) – has been selected. It consists of an indentation at the bottom of the vessel, where the disk-shaped stator is placed. The hollow rotor ring is then placed around it inside the vessel. This setup allows a flexible impeller design and guarantees a sufficient flow within the whole vessel.

In a next step, the number of stator teeth and the pole pair number have to be chosen. The outer diameter of the motor depends on the type of impeller. For the exterior rotor type, the impeller blades are directly mounted at the outer part of the rotor [cf. Fig. 2(b)]. The minimum blade length required is set to 20 mm, thus the outer diameter of the motor is limited to 130 mm. This implies that for this experimental setup the available space for the stator will be rather restricted. Therefore, only a setup with a small number of stator teeth is recommendable, since otherwise there is not enough space for the stator windings. Sufficient winding space yet is required, since the torque directly depends on the coil current (cf. section III) and a certain maximal current

density shall not be exceeded. The minimum number of coils for a stable magnetic bearing is four, thus at least four stator teeth are needed. Such a setup would show single-phase characteristics and comparably large cogging torque. Setups with five or more stator teeth would also be possible. However, the setup with five stator teeth results in unbalanced passive bearing forces, thus high control currents are required. The setups with six or more stator teeth already limit the winding space significantly. These considerations lead to the selection of a motor with four stator teeth despite its aforementioned disadvantages. With a pole pair number of six, this setup can produce both torque and bearing forces with only four coils, as will be described in the next section.

## III. TORQUE AND BEARING FORCES

The motor setup was defined to consist of an exterior rotor type with a pole pair number of six and a stator teeth number of four. The rotor consists of twelve permanent magnets that are radially magnetized in alternating order (cf. Fig. 3). Four stator coils (one per stator teeth) have to produce both torque and bearing forces. Each coil can produce a radial force (often referred to as Maxwell force) and a tangential force (often referred to as Lorentz force). The right combination of these forces then allows to combine drive and bearing in one stator [10]. The required current excitation can be examined separately for torque and bearing forces and will be superimposed in the control commands. This concept of combined coils (no separate drive and bearing coils) is advantageous in terms of reducing the total required current, thus reducing copper losses [11].

The control algorithm for both torque and bearing forces requires permanent knowledge about the angular position of the rotor. Therefore, angular position sensors measure the magnetic field of the rotor in order to determine its position. This angular position is measured in the unit of an electrical angle, which is defined as the product of the mechanical angle times the pole pair number $p$:

$$\alpha_{elec} = p \cdot \alpha_{mech}. \qquad (1)$$

### A. Motor torque

This motor topology shows single-phase characteristics, thus there is a position, where no torque can be produced [cf. Fig. 3(a)]. Moreover, this setup provokes a cogging torque that interferes with the active motor torque. These inconveniences can be overcome by slight topology modifications that disturb the symmetry or by temporarily displacing the rotor out of its center position. However, there will always be a remaining cogging torque which might lead to jerky rotation at very low speeds.

The four stator coils have to be fed with a sinusoidal excitation current being in-phase with the electrical angle. Two opposite coils are in-phase, whereas they are phase-shifted by 180° with the remaining two coils, thus leading to a stator field pole pair number of two. All four coils then

produce radial forces that annihilate each other. However, the tangential forces result in a motor torque, which oscillates with the square value of a sine wave when rotating with a sinusoidal drive current applied. For a torque-current factor $k_T$ of one coil, the number of windings per coil $N_{coil}$ and the peak value of the drive current $\hat{I}_{drv}$ in one coil, the overall motor torque is given by

$$T(\alpha_{elec}) = 4 \cdot k_T \cdot \sin^2(\alpha_{elec}) \cdot N_{coil} \cdot \hat{I}_{drv}. \qquad (2)$$

Fig. 3(b) shows the rotor position for which the highest possible torque can be achieved (for $\alpha_{elec}$= 90°).

*B.   Bearing forces*

The rotor of the bearingless motor has to be stabilized in six degrees of freedom. One degree of freedom is the rotation that is controlled with the drive currents. Therefore, the magnetic bearing has to stabilize the five remaining degrees of freedom. With the disk-shaped rotor type, only the radial displacements in *x*- and *y*-direction have to be controlled actively by applying bearing currents. The other three degrees of freedom (tilting and axial displacement) are stabilized passively [3].

*1.   Passive bearing forces*

Both axial and tilting deflections are stabilized passively by means of attracting reluctance forces. The rotor weight $m_R$ counteracts the axial force, thus this reluctance force has to be sufficiently high so that the rotor position is only lowered up to a moderate extent ($\Delta z$). Therefore, the requirement for the axial stiffness factor $k_z$ can be stated as

$$k_z > \frac{m_R \cdot g}{\Delta z}, \qquad (3)$$

where $g$ is the gravitational acceleration constant ($g$ = 9.81 m/s$^2$).

The tilting mainly depends on the ratio of motor diameter to machine length (or height respectively). A sufficient reluctance force against tilting disturbance is a key requirement for the proper functioning of the bearingless motor. It is obvious that for a fixed rotor setup, these reluctance forces grow with the available stator iron area that the permanent magnets can act on. From this point of view, it would be recommendable to enlarge the tooth tip opening angle (cf. section IV).

*2.   Active bearing forces*

The remaining two degrees of freedom regulate the radial position of the rotor. There are also passive reluctance forces acting in radial direction, yet they do not have a stable working point. When the rotor is slightly displaced from its center position, the radial reluctance forces become stronger on the side where the air gap is now smaller. Thus, the rotor is removed even further away from its center position until it touches the stator. Therefore, the radial displacement has to be regulated permanently with an active control. The bearing system consists of two separate phases. Each phase consists
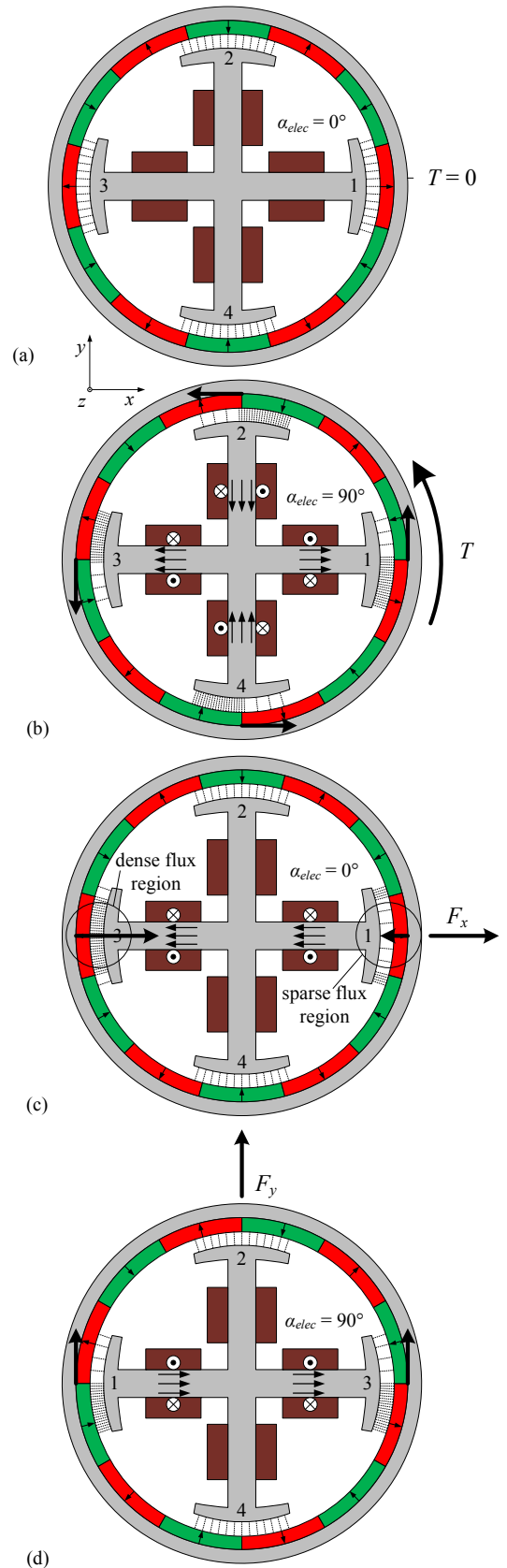


Fig. 3.   Excitation currents for torque (b) and bearing forces of one phase [(c) and (d)] in dependence on the rotor angle. For the rotor position in (a) no torque can be generated.

of two opposite coils, whereas these coils are phase shifted by 180°, thus leading to a stator field pole pair number of one. As depicted in Fig 3(c) and 3(d), such a coil arrangement (current feed shown in one phase) does not create torque, but bearing forces in *x*- and *y*-direction that depend on the rotor angle. For the considered phase

$$F_x(\alpha_{elec}) = 2 \cdot k_{F,x} \cdot \cos(\alpha_{elec}) \cdot N_{coil} \cdot \hat{I}_{bng} \qquad (4)$$

and

$$F_y(\alpha_{elec}) = 2 \cdot k_{F,y} \cdot \sin(\alpha_{elec}) \cdot N_{coil} \cdot \hat{I}_{bng} \qquad (5)$$

hold true, with the bearing-current factor per coil in *x*- and *y*-direction $k_{F,x}$ and $k_{F,y}$, respectively, the number of windings per coil $N_{coil}$, and a constant bearing current per coil $\hat{I}_{bng}$. In Fig. 3(c), the center of the right stator teeth faces the center of one magnet. In order to produce a force in this direction, the field on the right side has to be weakened, whereas it has to be fortified on the left side. Thus, the radial forces are used to center the rotor, whereas the tangential forces are zero in this angular rotor position. For an electrical angle of 90°, the center of the right stator teeth faces exactly the connection of two magnets [cf. Fig. 3(d)]. Both radial and tangential forces are created and their superposition results in a force in *y*-direction.

In combination with the second bearing phase, bearing forces in every desired radial direction can be generated for every possible angular rotor position. Displacement sensors determine the radial rotor position and feed it to the control algorithm. For a given required force, this control algorithm then calculates the bearing currents in dependence on the angular rotor position.

These active forces have to overcome the destabilizing radial stiffness (with factor $k_r$) in dependence on the maximal displacement $\Delta r_{max}$, leading to:

$$k_{F,overall}(k_{F,x}, k_{F,y}, \alpha_{elec}) > \frac{k_r \cdot \Delta r_{max}}{N_{coil} \cdot \hat{I}_{bng}}. \qquad (6)$$

## IV.    DESIGN AND OPTIMIZATION

Initial selection criteria have already defined the rough design parameters of the new motor topology. With 3D magnetostatic FEM simulations the optimal shape of the bearingless motor will be evaluated. The goal is to maximize the torque, to reduce cogging torque so that it is not dominating, and to achieve sufficient bearing forces (passively and actively). In a second step, the criteria for the optimal winding number will be derived.

### A.    Optimization Using 3D FEM

The design parameters are depicted in Fig. 4. The rotor consists of permanent magnets and a back iron ring. Therefore, the optimal thicknesses $\delta_m$ and $\delta_{bi}$, respectively, of these two elements have to be found. Moreover, this
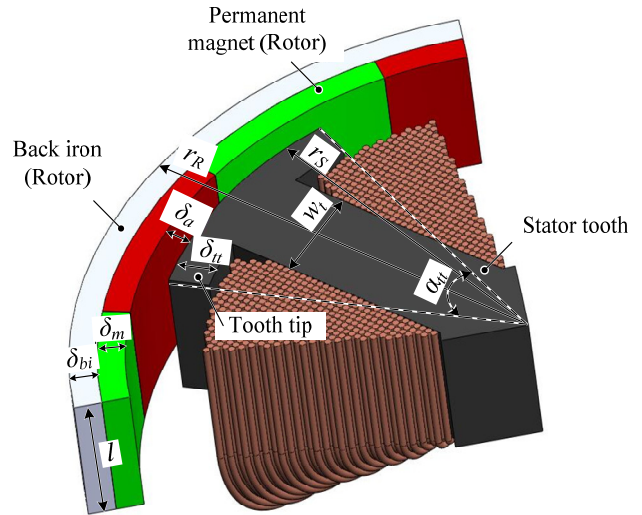


Fig. 4. A single stator tooth of the motor with its design parameters.

selection determines the diameter of the stator, since total machine diameter and air gap thickness are given. For the stator, the main parameters are the tooth width $w_t$, the tooth tip opening angle $\alpha_{tt}$ and the tooth tip thickness $d_{tt}$.

The size of the rotor (back iron and permanent magnets) and its ratio to the stator diameter significantly influence the torque. The achievable torque depends on the magnetic field in the air gap and the current in the windings. Therefore, a trade-off between these two factors has to be found. The first one (magnetic air gap field) is determined by the dimensions of the permanent magnets and by the applied winding current. Moreover, saturation effects have a high impact on this first factor. The second factor (winding current) mainly depends on the available size for the windings; it thus depends on the diameter of the stator and the shape of the stator teeth. A rotor thickness of 8 mm was found to be the optimal value, with the rotor equally distributed in magnet and back iron material.

The tooth tip opening angle is another key parameter for both torque and bearing forces. For the considered stator tooth/pole pair combination the opening angle can be chosen either rather small (open tooth), with the stator tooth covering about one pole, or rather large (closed tooth), thus covering about three poles. In between, when the opening angle of the tooth tip matches with one pole pair, the torque and bearing forces are much lower or even zero. In this case, the flux passes over the tooth tip without entering the stator tooth and neither torque nor active bearing forces are produced.The passive reluctance forces strongly depend on the tooth tip opening angle. As predicted in section III, these forces grow with a larger stator iron area in front of the magnets. Even though a larger angle is desired for the stabilization of the axial position and the tilting, it has a negative effect on the active magnetic bearing for the radial position. Since the destabilizing radial reluctance force is also enlarged, higher control currents are needed in order to counteract radial
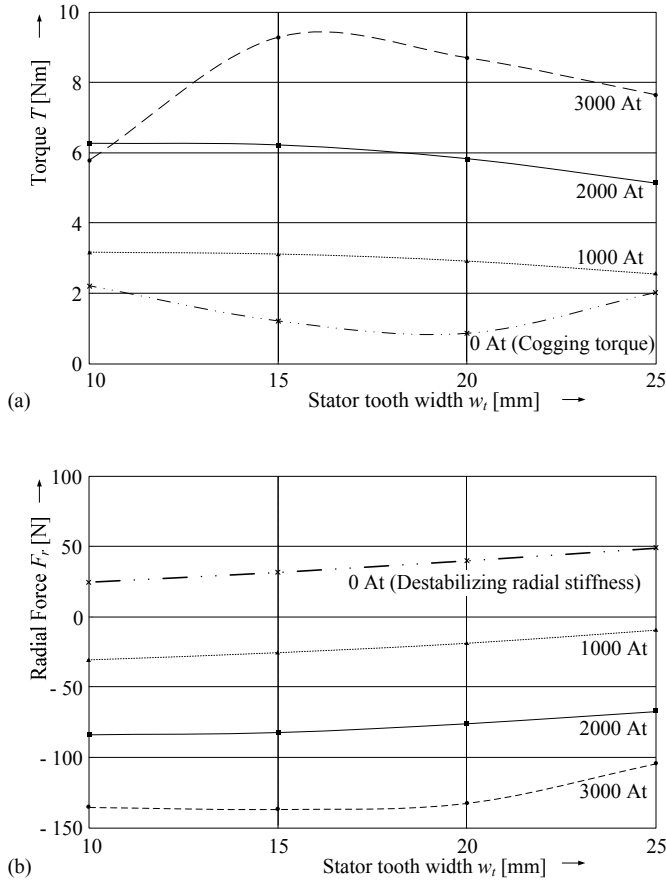
(a)



(b)

Fig. 5. Simulation results for torque and cogging torque (a) and for passive and active radial force for a radial displacement of 1 mm (b) in dependence on different stator tooth widths. The influence of the electrical excitation, measured in ampere-turns (defined as the product of winding number and coil current), is shown, whereby the value for 0 At represents the destabilizing passive radial force, which has to be overcome.

displacement. Moreover, it was shown that for the closed tooth stator type, only very little radial displacement can be handled by the magnetic bearing without leading to instability. An experimental setup revealed that for radial displacement of 1 mm, the magnetic fields are already extremely nonlinear and it is impossible to bring the rotor back to its center position. Therefore, only open tooth stator types will be considered in the following, since the CIP and SIP applications require that the bearing can deal with mechanical air gaps of at least 2 mm. The choice of the open tooth stator type also brings an advantage considering the cogging torque. The cogging torque varies with the angular rotor position. As a detailed analysis shows, for the case of open teeth, the cogging torque is minimal at a same angular position where no torque can be generated [cf. Fig. 3(a)] and it has its maximal value where sufficient torque can be produced to overcome the cogging torque inertia. Therefore, no additional measures have to be taken in order to start rotation. (This is different from the variant with closed teeth, where the maximal cogging torque appears at the angular rotor position of zero torque.)

TABLE I
OPTIMAL DESIGN PARAMETERS

| Parameter | Symbol | Value |
|---|---|---|
| Number of stator teeth | $q$ | 4 |
| Pole pair number | $p$ | 6 |
| Outer rotor diameter | $d_R$ | 130 mm |
| Air gap thickness | $\delta_a$ | 4 mm |
| Machine length | $l$ | 20 mm |
| Magnet thickness | $\delta_m$ | 4 mm |
| Back iron thickness | $\delta_{bi}$ | 4 mm |
| Outer stator diameter | $d_S$ | 106 mm |
| Stator tooth width | $w_t$ | 15 mm |
| Rated torque | $T$ | 6 Nm |
| Rated speed | $n$ | 500 r/min |

For the open tooth stator type, the optimal relation of stator tooth width, tooth tip opening angle and tooth tip thickness has to be evaluated. The simulations revealed that it is always optimal, when the tooth tip and the tooth itself have the same width. This actually means that we only consider stators with straight teeth and no tooth tips. Magnetic saturation is the cause of this geometric relation, as is also stated in [12].

The remaining parameter for the stator is its tooth width. Fig. 5(a) shows the resulting torque for a stator with different tooth widths, when the level of electrical excitation (magnetomotive force) is changed. This magnetomotive force is the product of the applied current and the number of windings per coil, with the unit of ampere-turn (At). It creates a magnetic field in the stator teeth that interacts with the magnetic field of the permanent magnets, which results in bearing forces and torque. As depicted in Fig. 5(a), the stator tooth width is preferably chosen small, however, a lower limit is given due to magnetic saturation. In Fig. 5(b), the bearing forces acting on the rotor are shown in case of radial displacement of 1 mm in positive x-direction. It can be seen that the resulting force is positive if zero current is applied, thus the rotor would even be displaced further away from its origin. Only with sufficient current applied, a negative force results that brings the rotor back to its center position. In order to minimize bearing currents, the tooth width should be chosen small. However, the remaining passive forces (axial stiffness and tilting) show the same behavior as the radial stiffness. Therefore, a larger tooth width is favorable and a minimal value is required to guarantee a stable passive bearing. With a tooth width value of 15 mm, high torque can be achieved, cogging torque is rather low [cf. Fig. 5(a)], and yet the bearing forces are sufficiently large.

The optimal design parameters found with the 3D-FEM simulations are summarized in Table I.

*B. Optimal winding number per coil $N_{coil}$*

There is a trade-off for the optimal winding number per coil $N_{coil}$ between the production of torque and force and dynamic considerations of the bearing.

According to (2), (4) and (5), the production of torque and force would require a large winding number in order to limit the necessary currents. However, (2), (4) and (5) are only

valid as long as no heavy saturation in the iron parts occurs. Therefore, it is useless to make the winding numbers excessively large.

For the dynamic considerations of the bearing, the electrical ($\tau_E$) and the mechanical time constant ($\tau_M$) have to be compared. The mechanical time constant is defined as

$$\tau_M = \sqrt{\frac{m_R}{k_r}} \ . \tag{7}$$

and thus dependent on the rotor mass $m_R$ and the radial stiffness factor $k_r$. The electrical time constant, given by

$$\tau_E = \frac{\hat{I}_{bng} \cdot L_{coil}}{U_{dc}} \tag{8}$$

with the peak value of the bearing current $\hat{I}_{bng}$, the inductance $L_{coil}$ of the coil, and the dc link voltage $U_{dc}$ (for bearing coils driven by an inverter in full bridge configuration), should be at least five times smaller than $\tau_M$ in order to achieve a stable bearing control. Therefore, from the viewpoint of control dynamics, a small value for $N_{coil}$ is preferable considering that $L_{coil}$ scales quadratically with $N_{coil}$.

## V.    EVALUATION WITH PROTOTYPE SETUP

Fig. 6 shows a prototype setup of the proposed topology. The four stator coils produce both torque and bearing forces.

Fig. 7 shows measurements of the four coil currents when the motor is rotating with a speed of about 375 r/min. Both drive and bearing currents are superimposed in each coil. When levitated, only very small bearing currents are necessary, thus the drive current is dominant. Ideally, the currents applied should thus be sinusoidal; however, the existing cogging torque is disturbing a smooth rotation. Moreover, magnetic asymmetries in the rotor disturb the sinusoidal shape of the coil currents, too.
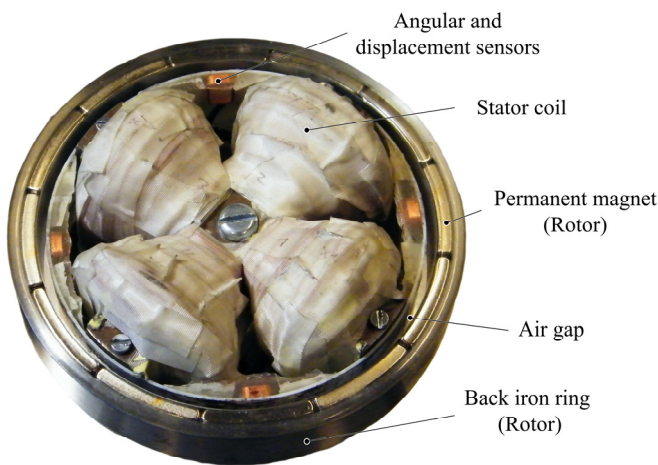


Fig. 6.  Prototype of the novel motor for bioreactor stirring applications.
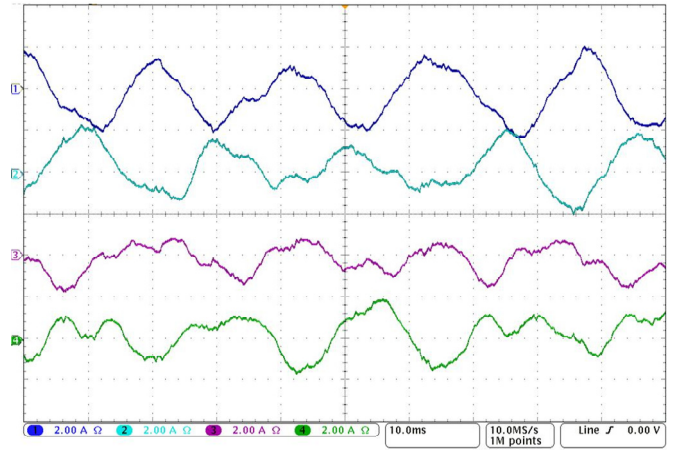


Fig. 7.  Measurements of the four coil currents during rotation with 375 r/min.  (Current-scale: 2 A/div., time-scale: 10 ms/div.)

## VI.    CONCLUSION

A novel motor topology with an exterior disk-shaped rotor with a pole pair number of six and a stator with four stator teeth has been introduced. Combined windings allow the generation of both motor torque and bearing forces in a very compact setup. This motor is especially suitable for delicate bioreactor stirring applications.

## REFERENCES

[1] J. Boehm, R. Gerber, J. R. Hartley and S. Whitley, "Development of active magnetic bearings for high speed rotors," IEEE Trans. Magn., vol. 26, no. , pp. 2544-2546, Sep. 1990.

[2] N. Watanabe, H. Sugimoto, A. Chiba, T. Fukao and M. Takemoto, "Basic characteristic of a multi-consequent-pole bearingless motor," in Proc. Power Convers. Conf.-Nagoya, 2007. PCC'07, Apr. 2-5, pp. 1565-1570.

[3] R. Schoeb and N. Barletta, "Principle and Application of a Bearingless Slice Motor," JSME international journal. Series C, Mechanical systems, machine elements and manufacturing, vol. 40, pp. 593-598, 1997.

[4] P. Karutz, T. Nussbaumer, W. Gruber, J. W. Kolar, „Novel Magnetically Levitated Two-Level Motor," IEEE/ASME Trans. Mechatronics, vol. 13, pp.658-668, 2008.

[5] T. Schneeberger, T. Nussbaumer and J. W. Kolar, "Magnetically Levitated Homopolar Hollow-Shaft Motor," IEEE/ASME Trans. Mechatronics, to be published.

[6] J. A. Asenjo and J. C. Merchuk, Bioreactor System Design, Marcel Dekker, Inc, New York, 1995.

[7] K. van't Riet and J. Tramper, Basic Bioreactor Design, Marcel Dekker, Inc, New York, 1991.

[8] S. S. Ozturk and W.-S. Hu, Cell culture technology for pharmaceutical and cell-based therapies, Taylor & Francis, Boca Raton, 2006.

[9] Y. Christi and M. Moo-Young, "Clean-in-place systems for industrial bioreactors: Design, validation and operation," Journal of Industrial Microbiology and Biotechnology, vol. 13, pp. 201-207, July 1994.

[10] S. Silber, W. Amrhein, P. Bösch, R. Schoeb, N. Barletta. "Design aspects of bearingless slice motors," IEEE/ASME Trans. Mechatron., vol. 10, no. 6, pp. 611-617, Dec. 2005.

[11] K. Raggl, T. Nussbaumer and J. W. Kolar, "Comparison of Winding Concepts for Bearingless Pumps," IEEE ICPE 07, pp. 1013-1020, Oct. 2007.

[12] P. Karutz, T. Nussbaumer, W. Gruber, J. W. Kolar, "Saturation Effects in High Acceleration Bearingless Slice Motors, " Proc. of the 2008 IEEE International Symposium on Industrial Electronics, pp. 472-477, Cambridge (UK), June 30 - July 2, 2008.